Supplementary Information

Vapochromism of Iridium(III) bis-terpyridine complex based on modulation of halide-to-ligand charge transfer transition

Shingo Hattori, Mio Kondo, Akiko Sekine and Kazuteru Shinozaki*

Graduate School of Nanobioscience, Yokohama City University, 22-2 Seto, Kanazawa-ku, Yokohama 236-0027 JAPAN

School of Science, Tokyo Institute of Technology, 2-12-1 O-okayama, Meguro-ku, Tokyo 152-8551 JAPAN

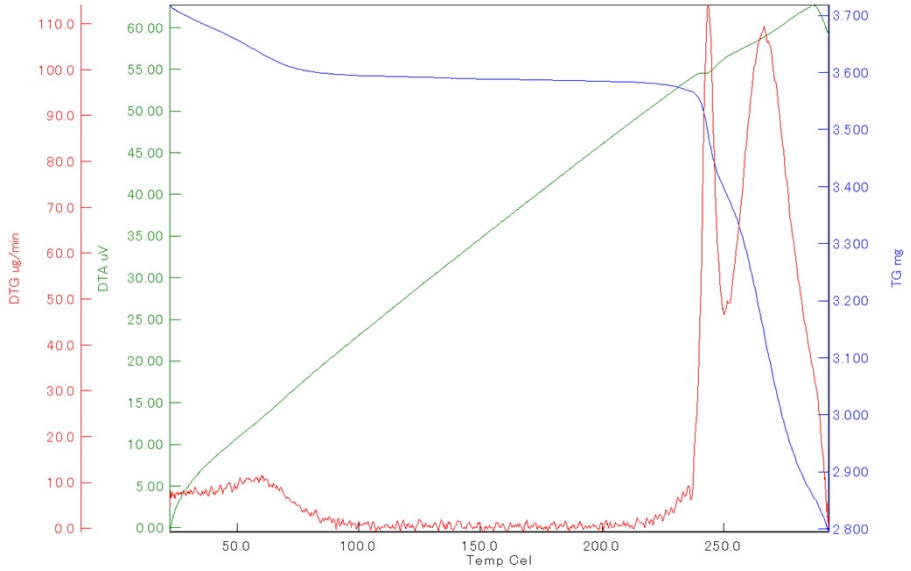

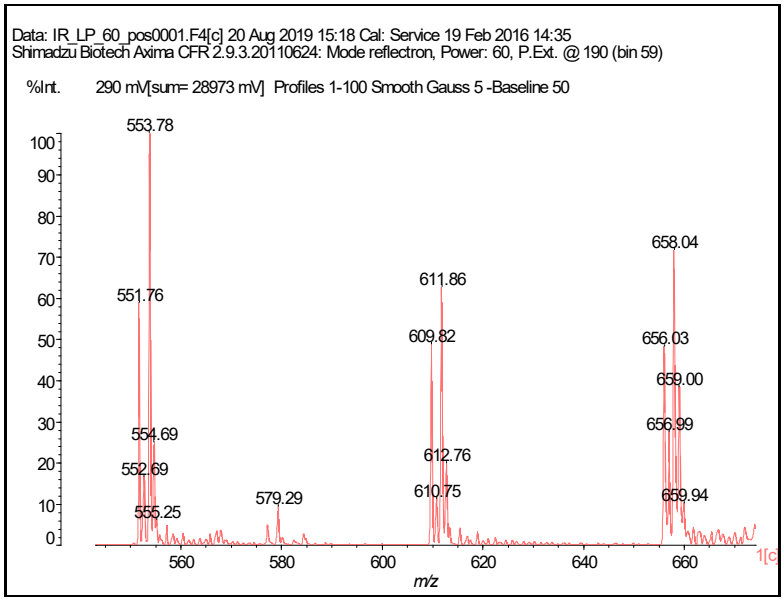

Fig. S1 (Top) A TG result (blue) for $[Ir(tpy)_2]I_3 \cdot 2H_2O$ along with DTG (red) and DTA (green). (Bottom) A MS spectrum for the sample heated at 570 K. Distinct three sets of doublets at *m*/*z* = 551.76 and 553.78 for $([Ir(tpy)]I+H)^+$, *m*/*z* = 609.82 and 611.86 for $([Ir(tpy)]_2I\text{-}H)^{2+}$, and *m*/*z* = 656.03 and 658.04 for $([Ir(tpy)_2]\text{-}H)^+$ are observed due to the isotopes of Ir atom (^{191}Ir and ^{193}Ir).

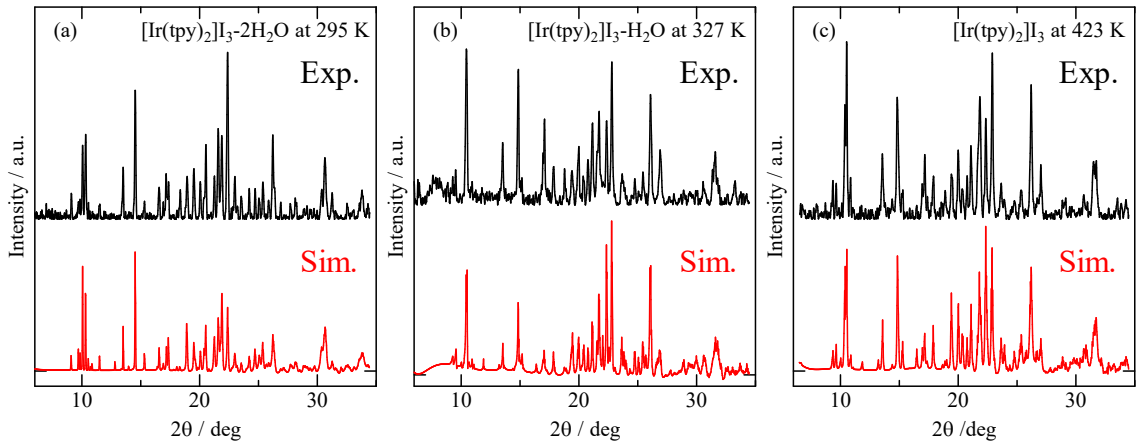

Fig.S2 XRD patterns measured at 295 (a), 327 (b), 423 K (c) and their simulated patterns obtained by RIETAN-FT[32] and VESTA[33] assuming the entire samples has the space group $P2_1/n$.

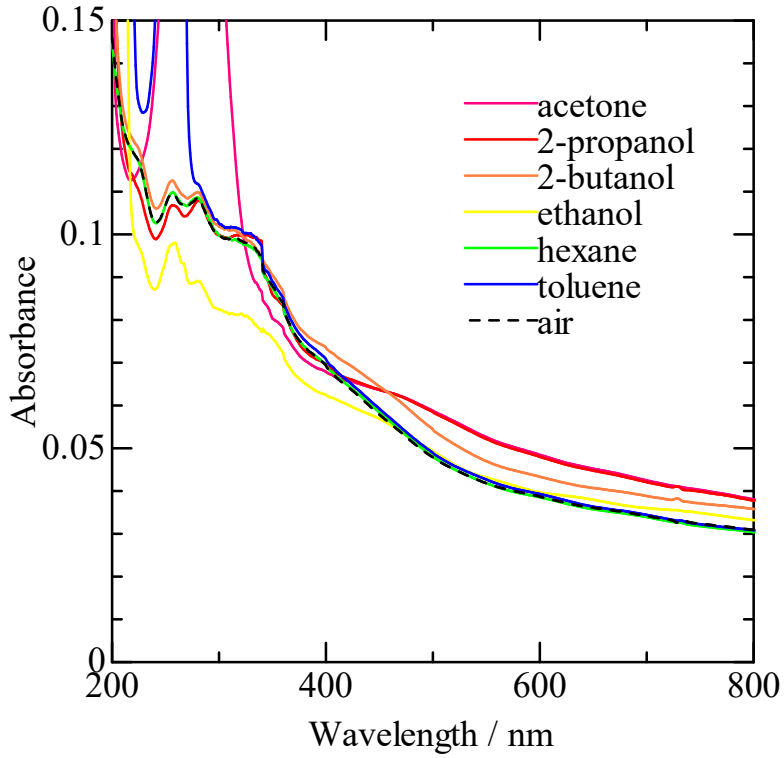

Fig. S3 Solid state absorption spectra for $[Ir(tpy)_2]I_3 \cdot 2H_2O$ after exposure to various organic vapors (pink: acetone, red: 2-propanol, orange: 2-butanol, yellow: ethanol, green: hexane, blue: toluene, black-broken: no solvent).

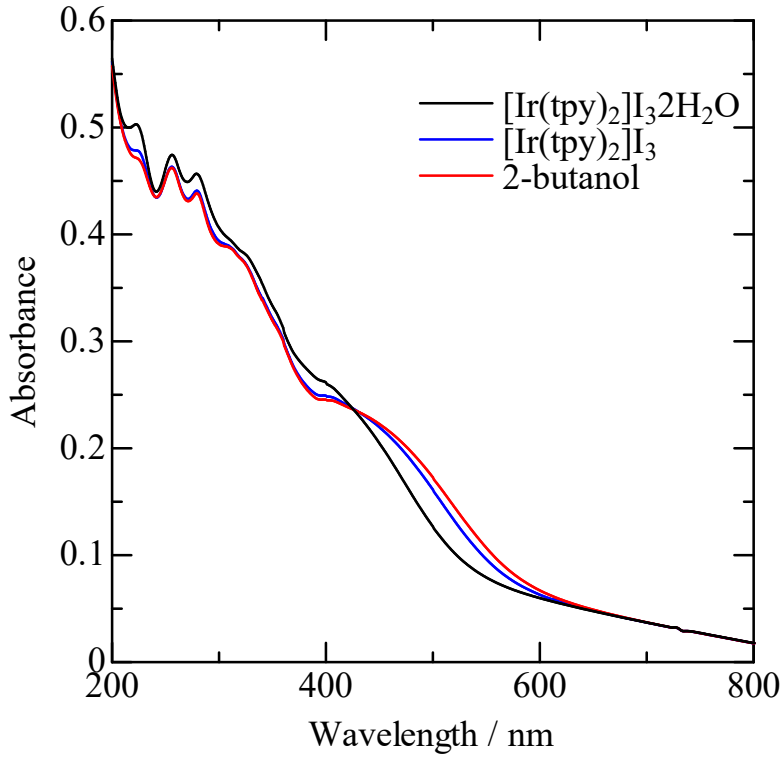

Fig. S4 A solid state absorption spectrum (red) for $[Ir(tpy)_2]I_3$ after exposure to dry 2-butanol vapor (red). Absorption spectra of $[Ir(tpy)_2]I_3 \cdot 2H_2O$ (black) and $[Ir(tpy)_2]I_3$ (blue) are exhibited for comparison. The XLCT peak wavelength in the red spectrum is estimated to be 487 nm.

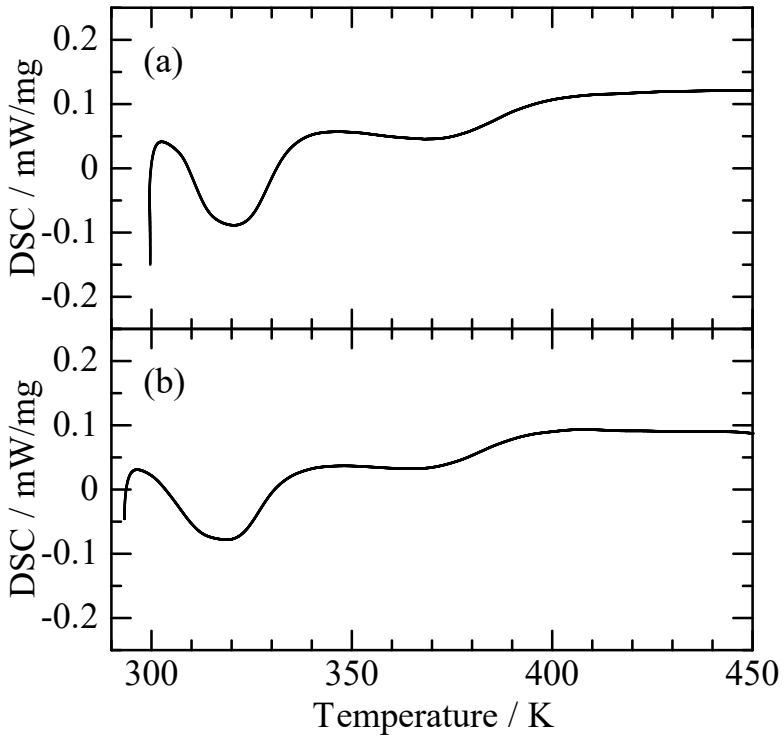

Fig. S5 DSC results for $[Ir(tpy)_2]I_3 \cdot 2H_2O$ (a) after exposure to NH_3 vapor (25% aq NH_3) and (b) without exposure to NH_3 vapor. Endothermic peaks for H_2O desorption are observed at 320 and 370 K for both the DSC curves, from which enthalpy changes for two H_2O desorption are evaluated as both ΔH = 56 mJ/mol (52 mJ/mg).

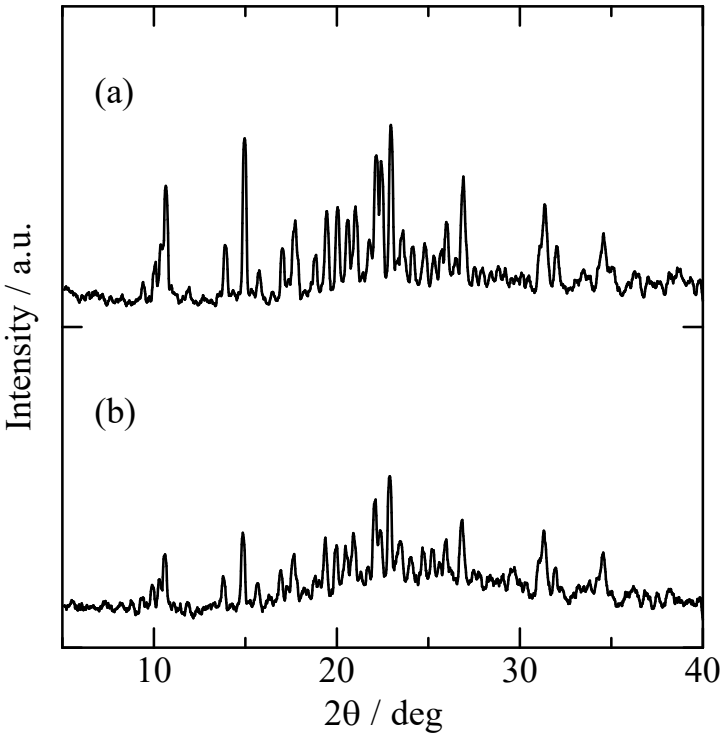

Fig. S6 PXRD patterns for $[Ir(tpy)_2]I_3 \cdot 2H_2O$ (a) before exposure to NH_3 vapor and (b) after exposure to NH_3 vapor (25% aq NH_3).

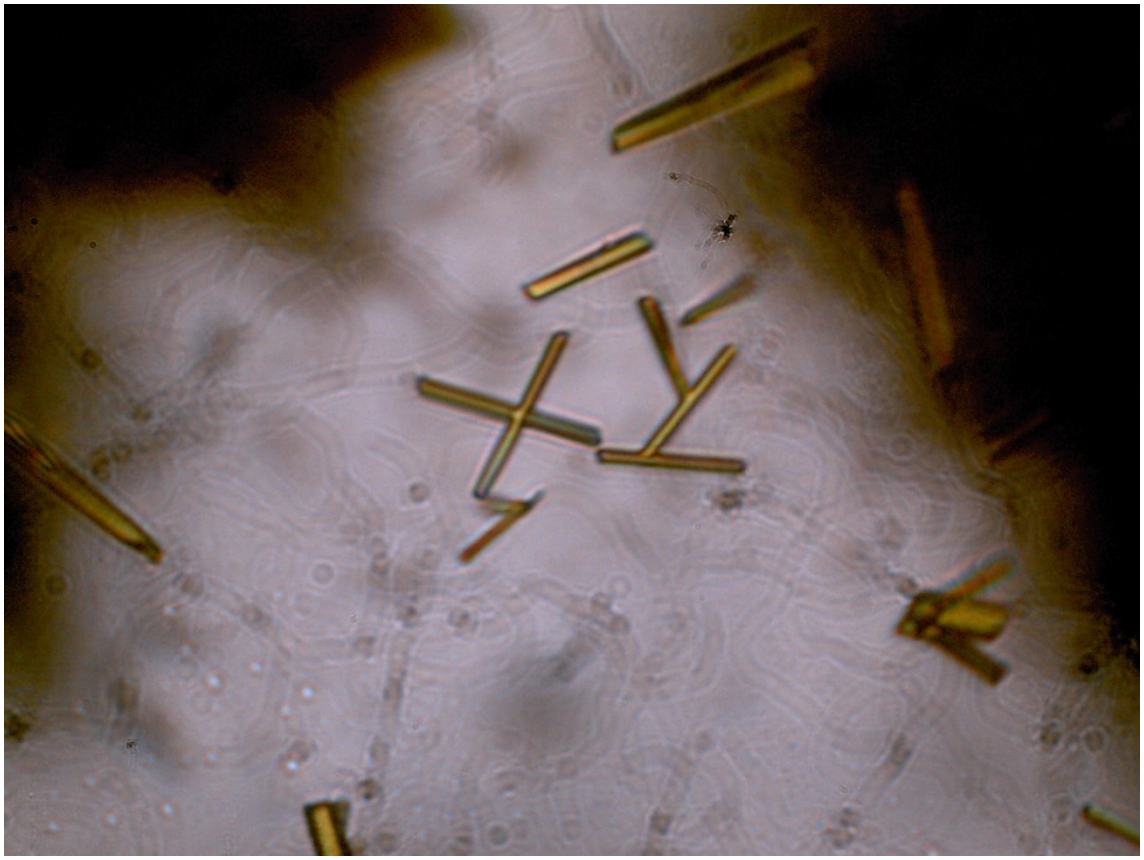

Fig. S7 A photograph of single crystal of $[Ir(tpy)_2]I_3\ 2H_2O$ (needle crystal, 0.5 mm×3.0 mm).

Table 1 X-ray crystallography of $[Ir(tpy)_2]I_3 \cdot 2H_2O$.

Temperature (K)	93
Crystal system	Monoclinic
Space group	$P2_1/n$
a (Å)	9.6383(18)
b (Å)	18.849(4)
c (Å)	17.787(3)
α (deg)	90
β (deg)	94.025(4)
γ (deg)	90
V (Å^3)	3223.5 (10)
λ(Mo $K\alpha$) (Å)	0.71075
Z	4
R	9.46

Table 2 Selected bond lengths [Å] and angles [º] of $[Ir(tpy)_2]I_3 \cdot 2H_2O$.

Ir-N1	2.030	N5-Ir-N6	80.9
Ir-N2	1.975	N1-Ir-N4	90.8
Ir-N3	2.071	N1-Ir-N5	102.8
Ir-N4	2.058	Ir-Ir	9.140
Ir-N5	2.007	Ir-Ir	10.243
Ir-N6	2.053	Ir-Ir	11.566
N1-Ir-N6	91.5	Ir-I1	5.156
N2-Ir-N4	104.0	Ir-I2	5.665
N2-Ir-N5	176.3	Ir-I3	5.336
N2-Ir-N6	96.8	I3-I3	5.044
N3-Ir-N4	92.2	O2-O2	5.266
N3-Ir-N5	96.8	I1-O1	3.743
N3-Ir-N6	92.6	I3-O2	3.628
N1-Ir-N2	80.1	I3-O2	3.664
N2-Ir-N3	80.3		
N4-Ir-N5	78.4		

Table 3 Cell lengths, cell angles, cell volumes for $[Ir(tpy)_2]I_3 \cdot nH_2O$ obtained by RIETAN-FP[33] and VESTA[34] assuming the entire samples has the space group $P2_1/n$.

	$[Ir(tpy)_2]I_3 \cdot 2H_2O$ (295K)	$[Ir(tpy)_2]I_3 \cdot H_2O$ (327K)	$[Ir(tpy)_2]I_3$ (423K)
a (Å)	9.7880(16)	9.472(3)	9.505(3)
b (Å)	19.248(4)	18.816(5)	18.719(5)
c (Å)	18.10883)	18.395(5)	18.278(5)
β (deg)	94.629(7)	95.924(3)	95.662(9)
V (Å^3)	3400.41	3261.07	3236.30